HADRON CANCER THERAPY COMPLEX EMPLOYING NON-SCALING FFAG ACCELERATOR AND FIXED FIELD GANTRY DESIGN

E. Keil*, CERN, Geneva, Switzerland, A.M. Sessler†, LBNL, Berkeley CA, USA
D. Trbojevic‡, BNL, Upton NY, USA

Abstract

Non-scaling FFAG rings for cancer hadron therapy offer reduced physical aperture and large dynamic aperture as compared with scaling FFAGs. The variation of tune with energy implies the crossing of resonances during acceleration. Our design avoids intrinsic resonances, although imperfection resonances must be, and can be, crossed. We consider a system of three non-scaling FFAG rings for cancer therapy with 250 MeV protons and 400 MeV/u carbon ions. Hadrons are accelerated in a common RFQ and linear accelerator, and injected into the FFAG rings at $v/c = 0.1294$. H+/C6+ ions are accelerated in the two smaller/larger rings to 31 and 250 MeV/68.8 and 400 MeV/u kinetic energy, respectively. The lattices consist of doublet cells with a straight section for RF cavities. The gantry with triplet cells accepts the whole required momentum range at fixed field. This unique design uses either high temperature super-conductors or super-conducting magnets reducing gantry size and weight. Elements with variable field at beginning and at end set the extracted beam at the correct position for a range of energies.

INTRODUCTION

Cancer proton therapy exists today in many medical facilities and many more are being built throughout the world. These facilities consist of cyclotrons (often a scaling FFAG) or synchrotrons. In this paper we consider non-scaling FFAG. The advantages of non-scaling FFAG with respect to synchrotrons are the fixed magnetic field and possibilities of higher repetition rates for spot scanning. With respect to cyclotrons the advantage is very much reduced magnet weight and ease of changing the final energy. Because of the possibility of changing energy and location with each spot (having a repetition rate of about 100 Hz) the cancerous tumor can be carefully scanned in three dimensions. We have worked on the subject before [1, 2].

ACCELERATOR COMPLEX

The facility consists of three rings with 36 cells each, circumferences 34.56 m, 43.2 m and 51.84 m, shown in Fig. 1. The cell lengths L_p, 0.96 m, 1.2 m, 1.44 m, are in the ratio 4:5:6. Tab. 1 shows the beam parameters. The maximum kinetic energies at extraction are 250 MeV for H+ and 400 MeV/u for C6+. In Ring 2, the values of $B\rho$ are the same for H+ and C6+. Acceleration changes them by a factor of three. All rings can be operated at constant excitation for both species. In Tab. 1, the particle speeds $c\beta$ are equal in the 1-Inj column of Ring 1 for H+ and in the 2-Inj column of Ring 2 for C6+ rings. Hence, both species can be accelerated in the same system of RFQ and linear accelerator. The lattices are very similar. Transfer of the bunches from the buckets in one ring to buckets in the next ring is possible, since all RF systems operate at 1.3 GHz.

Lattices

We adopt doublets of combined function magnets for focusing. The straight section space for the RF cavities, 0.3 m, and the gap between the magnets, 0.1 m, are the same in all rings. The phase advances stay well below the systematic half integral resonance at $q_1 = q_2 = 0.5$ at the lower edge of the energy range.

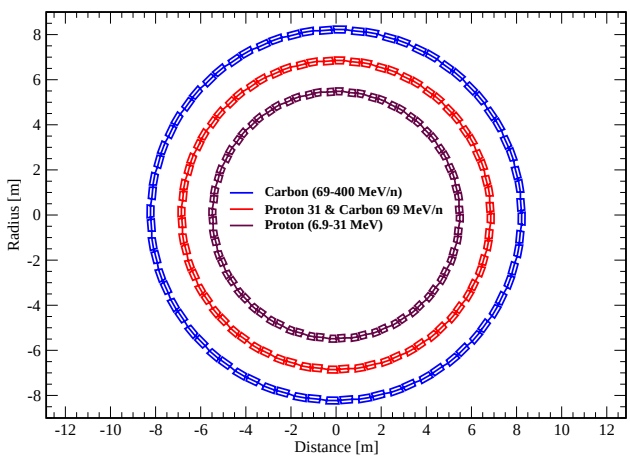

Figure 1: Schematic layout of the rings

We adjust the bending angles such that the path length variation Δs with $\delta p/p$ approximately vanishes to first order at the reference energy. Its remaining variation is predominantly quadratic. This is achieved by bending the beam away from the machine centre in the horizontally focusing F magnets [3]. The variation of the time of flight with $\delta p/p$ of the non-relativistic H+ and C6+ ions is dominated by the variation of their speed $c\beta$. All rings have similar lattice layout and orbit functions. Maximum β-functions and dispersion D are roughly proportional to L_p. In Ring 3, we have $\hat{\beta}_x \approx 2$ m, $\hat{\beta}_y \approx 2.3$ m, $\hat{D} \approx 86$ mm.

* Eberhard.Keil@t-online.de
† Work supported by the U.S. Department of Energy under Contract No. DE-AC02-05CH11231.
‡ Supported by the U.S. Department of Energy under Contract No. DE-AC02-98CH10886

Table 1: Beam parameters of H+ and C6+ in rings 1, 2, 3. Identical particle parameters at n-Extr and (n+1)-Inj.

Particle	H+				C6+			
Ring	1-Inj	1-Extr	2-Inj	2-Extr	2-Inj	2-Extr	3-Inj	3-Extr
Kin. en./u/MeV	7.951	30.97	30.97	250	7.8934	68.801	68.801	400
β	0.1294	0.2508	0.2508	0.6136	0.1294	0.3645	0.3645	0.7145
$B\rho$/Tm	0.4083	0.8107	0.8107	2.432	0.8107	2.432	2.432	6.3472

The vertical aperture radius A_y is determined by the amplitude of the vertical betatron oscillations. As in PIMMS [4], we assume normalised emittances $\varepsilon = 0.519\pi$ μm and $\varepsilon = 0.7482\pi$ μm for H+ and C6+, respectively. For a pessimistic estimate of A_y, we use the highest value of β_y in the acceleration range at distance s along a cell, and the lowest momentum error. We allow for three RMS beam radii within A_y. We calculate the contribution of the horizontal betatron oscillations to the horizontal aperture A_x in a similar manner. We then look for the maximum and minimum horizontal offsets x at distance s along a cell, and in the same ranges of $\delta p/p$. We subtract three times the horizontal RMS betatron beam radius from the minimum offset x to find the minimum horizontal aperture A_x, and add three times the horizontal RMS betatron beam radius to the maximum offset x to find the maximum horizontal aperture A_x. We arrive at the apertures of the F and D magnets shown in Tab. 4. Ring 3 has the largest aperture of the three rings, because the cells are the longest. The vertical aperture A_y in Ring 2 and the minimum horizontal aperture A_x are determined by the C6+ ions, while the maximum horizontal aperture A_x is due to the H+.

Table 2: RF system parameters at $f_{\rm RF} \approx 1.3$ GHz, initial and final harmonic numbers h_i and h_f, initial step $|\Delta h|$, number of turns, maximum circumferential voltage V

Ring		h_i	h_f	$\lvert\Delta h\rvert$	turns	V/MV
1	H+	1158	598	8	289	0.11
2	H+	747	298	25	116	2.4
2	C6+	1448	507	27	253	0.61
3	C6+	619	309	19	81	10.8

Acceleration

We adopt jumping the harmonic number h [5]. The energy gain in a turn ΔE is adjusted such that the change in $c\beta$ causes a change of the revolution period by an integral number of RF cycles, and hence corresponds to an integral step Δh in h. Since $\Delta\beta/\beta = -\Delta h/h$, and $\mathrm{d}\beta/\mathrm{d}\gamma = 1/\beta\gamma^3$, it follows that $\Delta E = -E_0\beta^2\gamma^3\Delta h/h$, where E_0 is the rest energy of the particle. Hence, the smallest ΔE is achieved with $\Delta h = -1$ and large h. At fixed Δh, ΔE increases rapidly during acceleration. Its variation can be reduced by starting acceleration with $|\Delta h| \gg 1$, gradually decreasing $|\Delta h|$, and switching to $\Delta h = -1$ towards the end. Tab. 2 shows the main parameters of the RF systems, and how h decreases during acceleration, since the revolution period decreases because of the increasing speed $c\beta$. The number of turns is significantly smaller than the difference $(h_i - h_f)$, because of the initial step $|\Delta h| > 1$, and much smaller than in a synchrotron. The energy gain per turn varies by less than a factor of two, but is much larger than in a synchrotron. The high rate of acceleration ensures fast crossing of the resonances. The bunches are arranged in a train. The train occupies a fixed time interval ΔT, which is a small fraction of the revolution period in Ring 1 and in Ring 2 for C6+. This fraction of the revolution period grows during acceleration.

Table 3: Extraction kicker parameters

Ring	2	3
Kick angle/mrad	10.7	6.1
Rise time/ns	80	80
Aperture width/mm	33	46
Aperture height/mm	21	15
Kicker length/m	0.2	0.2
Kicker field/T	0.13	0.19

Injection and Extraction

Extraction happens in two stages: (i) A full-aperture fast kicker magnet in the longer straight section deflects the extracted beam such that it is outside the circulating beam one or more cells downstream. The energy of the extracted beam can be varied in steps at most equal to the voltage V in Tab. 2 by accelerating for a variable number of turns. We operate all rings with about 200 bunches, and leave about 1/3 of the circumference free for the extraction kicker rise time in Ring 3 and Ring 2 for H+. There, the extraction kickers have the most demanding parameters shown in Tab. 3. The extraction kicker in Ring 1 and all injection kickers have longer rise times. (ii) A septum magnet deflects the extracted beam further, such that it misses components downstream, and sends it into a transfer line. Injection uses similar components in reverse order.

Table 4: Magnet parameters, aperture in mm, field B in T.

Magnet	F			D		
Ring	1	2	3	1	2	3
Min hor apert	-12	-16	-23	-6	-9	-8
Max hor apert	12	22	34	6	12	20
B at min apert	-0.5	-0.9	-1.9	0.8	1.6	3.2
B at max apert	-0.3	-0.4	-0.6	0.7	1.3	2.6
Vert half apert	5	8	6	8	12	8

Magnets

Tab. 4 shows the apertures and the fields of the combined function magnets, assumed to be sector magnets. The minimum and maximum values of the horizontal aperture in the F and D magnets are calculated from tables in the manner discussed in the section above. The gradients in the combined function dipoles cause a variation of the magnetic field across the horizontal aperture, quantified in the rows labelled Field at min/max hor aperture. The fields do not change sign inside the horizontal aperture.

In Ring 1, the fields are below 1 T. The maximum field in Ring 2, 1.6 T, occurs in the D magnets at the minimum horizontal aperture, i.e. at its radially inside edge. The magnets in these rings are conventional iron-dominated magnets. They may be excited either by resistive room-temperature coils, or by coils made of high-temperature super-conductor [6]. The maximum field in Ring 3 also occurs in the D magnets at the minimum horizontal aperture. At about 3.2 T, it is in the range of easy super-conducting magnets. Suitable combined function magnets can be arrived at by scaling from the super-conducting magnets in the proposed proton transport line for the J-PARC neutrino experiment [7].

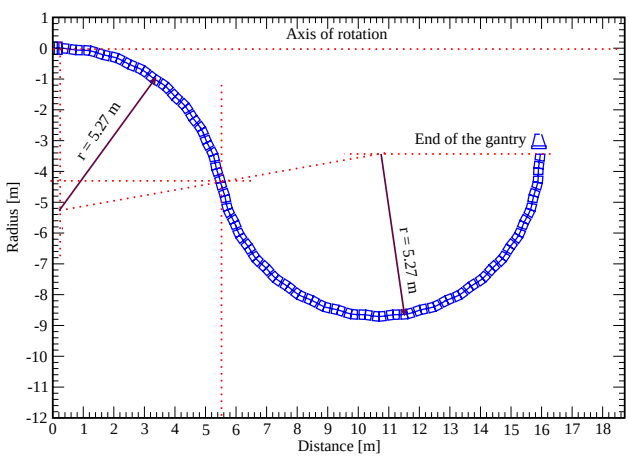

Figure 2: Schematic layout of the gantry

GANTRY

The beam is assumed to have equal emittances $\varepsilon_x = \varepsilon_y$. In the fixed transport line from the accelerators to the rotating gantry, it is matched to equal β-functions, $\alpha_x = \alpha_y = 0$, and $D_x = D'_x = 0$ at the junction. A 0.3 m long straight matching insertion consists of two quadrupoles and two drift spaces, and rotates with the gantry. It matches the round beam at the end of the transfer line to the gantry cells at any rotation angle. The gantry cells consist of non-scaling FFAG cells of combined function dipoles, arranged in the order FDDF. The bending angle of a cell is $\pm\pi/18$. The bending angles of the F and D magnets are adjusted such that $D_x = D'_x = 0$ at the centre of the D magnet. There, the curvature can be changed without harm to the matching of β-functions and dispersion D_x at $\Delta p/p = 0$. At the reference energy with $\delta p/p = 0$, the maximum β-functions are less than 1.63 m. The dispersion varies in the range $0 \leq D_x \leq 55$ mm. Fig. 2 shows a schematic layout. The first eight cells bend the beam away from the axis of rotation. The remaining seventeen cells have the opposite curvature, and bend the beam back towards the axis of rotation. The distance between the end of the gantry and the axis of rotation, as well as the maximum distance between the gantry and the axis of rotation, about 9 m in Fig. 2, can be varied by changing the number of cells. A similar gantry is in [8]. The gantry can transport particles with momentum errors up to $\delta p/p = \pm 0.2$. With one excitation of the magnets it transports C6+ ions with kinetic energies between 195 and 400 MeV/u. With about 40% of that excitation it transports H+ with kinetic energies between 118 and 250 MeV. A system of deflecting and focusing magnets at the end of the gantry compensates for lateral beam offsets, allows scanning, and achieves the desired beam size.

CONCLUSIONS

In this paper we have exhibited a design of a non-scaling FFAG and fixed field gantry. We have designed a series of rings producing 250 MeV protons or 400 MeV carbon, designed an acceleration scheme, considered injection and extraction, developed a matched into the gantry, and presented a compact gantry design. The complex facility design is now ready for detailed engineering and costing.

REFERENCES

[1] E. Keil, A.M. Sessler, D. Trbojevic, PAC (2005) 1667.

[2] D. Trbojevic, E. Keil, A. Sessler, Pres. at Internat. Symp. on Utilisation of Accel., 5 to 9 June 2005, Dubrovnik, Croatia.

[3] E. Keil, A.M. Sessler, Nucl.Instr.Meth. **A538** (2005) 159.

[4] P.J. Bryant (ed.), CERN-2000-006, Vol. 2 (2000).

[5] A.G. Ruggiero, BNL Doc. C-A/AP/237 (2006)

[6] R. Gupta et al., PAC (2005) 3018.

[7] T. Nakamoto et al., PAC (2005) 495.

[8] D. Trbojevic et al., EPAC (2006) WEPCH180.